

# Conformational Plasticity and Dynamics in the Generic Protein Folding Catalyst SlyD Unraveled by Single-Molecule FRET

Dana Kahra<sup>1</sup>, Michael Kovermann<sup>2</sup>, Christian Löw<sup>3</sup>, Verena Hirschfeld<sup>1</sup>,  
Caroline Haupt<sup>2</sup>, Jochen Balbach<sup>2</sup> and Christian Gerhard Hübner<sup>1\*</sup>

<sup>1</sup>*Institut für Physik, Universität zu Lübeck, Ratzeburger Allee 160, D-23564 Lübeck, Germany*

<sup>2</sup>*Institut für Physik, Biophysik, Martin-Luther-Universität Halle-Wittenberg, D-06099 Halle (Saale), Germany*

<sup>3</sup>*Department of Medical Biochemistry and Biophysics, Karolinska Institutet, SE-17177 Stockholm, Sweden*

*Edited by C. R. Matthews*

## Keywords:

conformational dynamics;  
enzyme catalysis;  
protein folding;  
single molecule

The relation between conformational dynamics and chemistry in enzyme catalysis recently has received increasing attention. While, in the past, the mechanochemical coupling was mainly attributed to molecular motors, nowadays, it seems that this linkage is far more general. Single-molecule fluorescence methods are perfectly suited to directly evidence conformational flexibility and dynamics. By labeling the enzyme SlyD, a member of peptidyl-prolyl *cis-trans* isomerases of the FK506 binding protein type with an inserted chaperone domain, with donor and acceptor fluorophores for single-molecule fluorescence resonance energy transfer, we directly monitor conformational flexibility and conformational dynamics between the chaperone domain and the FK506 binding protein domain. We find a broad distribution of distances between the labels with two main maxima, which we attribute to an open conformation and to a closed conformation of the enzyme. Correlation analysis demonstrates that the conformations exchange on a rate in the 100 Hz range. With the aid from Monte Carlo simulations, we show that there must be conformational flexibility beyond the two main conformational states. Interestingly, neither the conformational distribution nor the dynamics is significantly altered upon binding of substrates or other known binding partners. Based on these experimental findings, we propose a model where the conformational dynamics is used to search the conformation enabling the chemical step, which also explains the remarkable substrate promiscuity connected with a high efficiency of this class of peptidyl-prolyl *cis-trans* isomerases.

## Introduction

Beside many proteins and protein domains, which fold into their native structure within microseconds to seconds, there is a number of proteins where *cis-trans* isomerization of peptidyl-prolyl bonds can become the rate-limiting step and therefore can retard such fast conformational folding reactions.<sup>1</sup> Polypeptide chains not having attained their fully native structure are prone to aggregation,<sup>2</sup> which limits the efficiency of formation of functional

---

\*Corresponding author. E-mail address:  
[huebner@physik.uni-luebeck.de](mailto:huebner@physik.uni-luebeck.de).

Abbreviations used: PPIase, peptidyl-prolyl *cis trans* isomerase; FKBP, FK506 binding protein; smFRET, single-molecule fluorescence resonance energy transfer; TtSlyD, SlyD from *Thermus thermophilus*; EcSlyD, *Escherichia coli* SlyD; IF, inserted-in-flap.

proteins. Nature has evolved several strategies to overcome these limitations. A class of enzymes, the peptidyl-prolyl *cis-trans* isomerases (PPIases), catalyzes the slow *cis-trans* isomerization reaction of prolyl peptide bonds,<sup>3-5</sup> and molecular chaperones prevent unfolded or partially folded peptide chains from aggregation.<sup>6</sup>

One of the best-studied families of PPIases is the FK506 binding protein (FKBP) family, of which the members are characterized by high substrate specificity.<sup>7</sup> In several proteins, like for example, trigger factor,<sup>8-10</sup> SurA,<sup>11,12</sup> FkpA<sup>13</sup> or MtFKBP17,<sup>14</sup> the PPIase domain is complemented by a chaperone domain, lowering substrate specificity while giving rise to a dramatic increase in catalytic efficiency, rendering them generic catalysts for protein folding.<sup>15,16</sup>

SlyD is a member of this family and is present among all prokaryotes.<sup>17</sup> It consists of two structurally well-separated domains: the N-terminal prolyl isomerase domain of FKBP type with the second domain integrated in the FKBP flap ("inserted-in-flap" (IF) domain)<sup>14,18,19</sup> and an unstructured C-terminal tail of variable length, rich in cysteine and histidine residues with high affinity to metal ions. The chaperone activity resides in the IF domain because deletion of that domain results in loss of this activity.<sup>18,19</sup> Compared to related FKBP prolyl isomerases and to the isolated FKBP domain, the PPIase activity of SlyD is enhanced by a factor of

about 100 in the presence of the chaperone domain.<sup>15,16,19</sup>

It was hypothesized that the coupled transfer of substrate proteins bound at the chaperone domain to the PPIase domain could be responsible for this increase in PPIase activity.<sup>15,16,18</sup> However, direct evidence for this domain communication presumably by conformational dynamics of the two domains relative to each other was lacking.

Here, we set out to directly monitor the conformational heterogeneity and dynamics of full-length SlyD from *Thermus thermophilus* (*Tt*SlyD) (Fig. 1a), which is the shortest member of the SlyD family, by single-molecule fluorescence resonance energy transfer (smFRET) experiments in conjunction with fluorescence correlation analysis in order to elucidate how the conformational dynamics supports catalysis.

smFRET experiments with a confocal microscope in solution indicate conformational heterogeneity of *Tt*SlyD with two major conformational states. This is in agreement with NMR structural analysis of *Escherichia coli* SlyD (*Ec*SlyD) showing no distinct orientation of the two domains relative to each other.<sup>18,20</sup>

A sophisticated correlation analysis unraveled conformational dynamics on the millisecond time-scale. Comparison with extensive Monte Carlo simulations allowed us to demonstrate conformational heterogeneity beyond a model where only

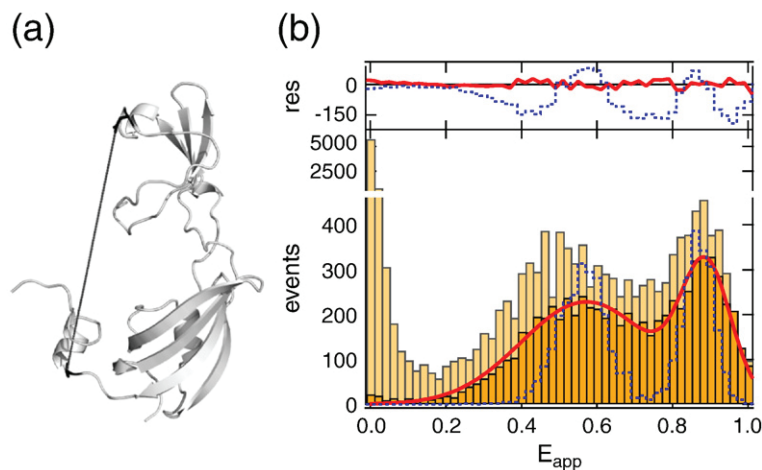


**Fig. 1.** (a) Three-dimensional structure of *Tt*SlyD<sup>19</sup> derived from X-ray crystallography, comprising the IF domain (top) and the FKBP domain (bottom). The positions for cysteine substitutions for dye insertion are emphasized in dark gray (T139 and D82). The distance (gray line) of the labeling positions out of this structure is  $d = 47 \text{ \AA}$ , resulting in an energy transfer efficiency of  $E_t = 0.62$  for the employed dye pair. (b) Burst-wise FRET analysis of the doubly labeled *Tt*SlyD excited by continuous-wave laser light at 488 nm (40  $\mu\text{W}$ ) and by pulsed laser light at 635 nm (15  $\mu\text{W}$ ,

10 MHz). (Bottom) Histogram of the number of bursts with the particular apparent transfer efficiency  $E_{app}$  calculated from the uncorrected data (filled bars). The bursts are selected either by only one sum threshold of 40 cts/ms for the total intensity during donor excitation (light yellow) or by an additional threshold of 10 cts/ms for acceptor intensity after direct excitation (dark yellow). In the latter case, the burst events caused by donor-only labeled molecules are suppressed efficiently. The shape of the remaining histogram is not modified except for a small shift to higher  $E_{app}$  values, indicative for bleaching events, which are also suppressed. The complete histogram, calculated with the two thresholds (dark yellow), was fitted to a two-Gaussian model (red line), determining the center positions of  $\langle E_{app,1} \rangle = 0.56$  and  $\langle E_{app,2} \rangle = 0.88$  for the possible two main populations. Overlaid histogram of predicted values from a shot-noise-limited simulation using the two fixed apparent mean FRET efficiencies  $\langle E_{app,1} \rangle$  and  $\langle E_{app,2} \rangle$ , which are populated equally (blue dotted line). (Top) Residuals of the experimental data to the fit model (red line) and to the simulated distribution (blue dotted line).

two conformations are exchanging. Our findings allowed us to propose a mechanism by which heterogeneous dynamics support the enzymatic function of a protein.

## Results

### Protein labeling and characterization

To monitor a possible relative domain motion of *TtSlyD*, we labeled each of the two domains with one reporter dye. Two solvent-exposed residues (D82 and T139) were exchanged by cysteines, which are conjugated with the thiol-reactive maleimide dyes Alexa Fluor 488 as donor and Atto 647N as acceptor. The dye pair was chosen based on the distance of about 47 Å between the C<sup>α</sup> atoms of D82 and T139 in the crystal structure of *TtSlyD*<sup>19</sup> (Fig. 1a). The Förster radius accounts to  $R_0 = 51$  Å (Supporting Text S1.1), well suited to study distance changes between the two domains.

The labeling efficiency was tested by different methods. Mass spectrometry revealed no detectable population of unlabeled or singly labeled molecules (data not shown). For the doubly labeled protein, absorption spectroscopy and burst analysis on the single-molecule level (Fig. S3) yielded more quantitative results indicative of a ratio of 2.8:1:0.5 between acceptor-only, acceptor-donor and donor-only labeled molecules.

To test for possible unspecific attachment of the dye by hydrophobic interactions, we unfolded the labeled protein sample at a concentration of 6 M GdmCl, run it through a filter unit in a centrifuge and refolded it, not giving rise to any change in the transfer efficiency ( $E_t$ ) histogram (Fig. S2).

Interactions of the dyes with the protein were further analyzed by fluorescence lifetime and time-resolved fluorescence anisotropy measurements on singly labeled single cysteine variants (D82C or T139C). Only negligible changes in the fluorescence characteristics were found (Supporting Text S2.2–S2.4).

The PPIase activity of the different *TtSlyD* variants was examined by a standard refolding assay of the reduced and carboxymethylated variant of RNase T1 S54G/P55N (RCM-T1).<sup>17</sup> The refolding activity of the doubly labeled *TtSlyD* is only marginally reduced to about  $(80 \pm 10)\%$  of the activity of wild-type *TtSlyD*. The large error figures result from the difficult spectroscopic determination of the exact protein concentration of the labeled *TtSlyD*. The catalytic activity of the doubly labeled *TtSlyD* used for the smFRET experiments is still 2 orders of magnitude above *TtSlyD* lacking the complete IF domain (*TtSlyD*ΔIF) (Table S1).

### smFRET reveals conformational heterogeneity

Figure 1b shows the histogram of the apparent energy transfer efficiencies  $E_{app}$  of fluorescence bursts measured under native conditions of apo-*TtSlyD*, calculated according to

$$E_{app} = \frac{I_A}{I_A + I_D} \quad (1)$$

where  $I_A$  and  $I_D$  are the detected acceptor and donor fluorescence intensities, which can be corrected for the fluorescence quantum yields of the dyes and the detection efficiencies (Supporting Text S1.4) to yield the actual transfer efficiency  $E_t$  that is related to the donor–acceptor distance  $r$  by

$$E_t = 1 / \left( 1 + (r/R_0)^6 \right) \quad (2)$$

where  $R_0$  is the Förster radius<sup>21</sup> being the distance where half of the excitation quanta are transferred to the acceptor, which is related to the properties of the dyes and the medium via

$$R_0 = 0.211 (\phi_D \kappa^2 n^{-4} J_{AD}(\lambda))^{1/6} \quad (3)$$

Here,  $\phi_D$  is the quantum yield of donor dye,  $\kappa^2$  is the orientational factor,  $n$  is the refractive index and  $J_{AD}(\lambda)$  is the overlap integral between donor emission and acceptor absorption spectra.<sup>22</sup>

The histogram covers a rather broad range from  $E_{app} = 0.3$  up to  $E_{app} = 1.0$ , which cannot be fitted with a single Gaussian distribution. The minimal model that allows for satisfactory fitting of the  $E_{app}$  histogram measured with *TtSlyD* is made up of two Gaussians (Fig. 1b). While this finding would at a first glance imply that two unique, distinct conformational states of *TtSlyD* exist, the question remains whether the width of the two Gaussians can be explained by photon shot noise, that is, by the limited number of stochastically emitted photons. To answer this question, we compare the experimentally obtained distribution with a simulated distribution taking the beforehand determined mean FRET efficiencies  $\langle E_{app,1} \rangle = 0.56$  and  $\langle E_{app,2} \rangle = 0.88$  from the two-Gaussian fit as input values. The measured  $E_{app}$  distribution is clearly broader than this simulated distribution (Fig. 1b). Shot-noise-limited performance of the setup was tested by single-molecule measurements of  $E_{app}$  distributions on polyproline 20 ((Pro)<sub>20</sub>), labeled with the same donor and acceptor dyes (Supporting Text S2.1). We can conclude that shot noise is not sufficient to explain the width of the  $E_{app}$  distribution.

On the other hand, photophysical and photochemical effects and hindered rotational freedom of the attached dyes may have an impact on  $R_0$  and the measured fluorescence intensities, respectively, thus potentially broaden the observed  $E_{app}$  distribution.

Detailed data analysis and control experiments showed, however, that these effects can be excluded from being responsible for the broadening of the transfer efficiency distribution (Supporting Text and Figures). We infer that the extra width must be related to the conformation of the protein. A merging of the two transfer efficiency peaks corresponding to the two hypothesized conformational states could indicate an exchange of the two conformations on the timescale of the integration time, which is 1 ms here. We therefore set out to study possible conformational dynamics of the enzyme.

### Conformational dynamics by correlation analysis

In order to assess possible dynamics of interconversion between the conformational states disclosed by FRET analysis, we followed an approach based on correlation functions, which was introduced by Torres and Levitus.<sup>23</sup> For that, the autocorrelation and cross-correlation of the fluorescence intensity fluctuations normalized by the square of the mean fluorescence intensity is calculated. The method of Torres and Levitus is based on the concept that the diffusion of the protein through the confocal volume leads to correlated fluctuations of both the donor and the acceptor fluorescence intensities, whereas conformational dynamics results in an anticorrelation of both signals. Because the diffusion part is identical in the autocorrelation function of, for example, the donor denoted as  $G_{GG}$  (referring to its emission color green) and in the donor-acceptor cross-correlation function denoted as  $G_{GR}$  (referring to the donor and acceptor emission colors green and red), the dynamics term can be extracted by division of both correlation functions ( $G_{GG}/G_{GR}$ ).

We calculated the correlation functions from burst-selected single-photon data. With the pulsed overlaid excitation scheme<sup>24</sup> (Supporting Text S1.3), we can exclude effects of acceptor photobleaching, which would also contribute a term to the correlation function that is not related to diffusion and would thus jeopardize the dynamics analysis<sup>25</sup> (Supporting Text S2.5). Furthermore, burst selection allows for suppressing the effects of the wavelength dependency of the focus size in the different detection channels.

However, burst selection prohibits the straightforward analysis of  $G_{GG}/G_{GR}$  in an analytical manner as proposed by Torres and Levitus<sup>23,26,27</sup> because the burst length is restricted in multiples of the bin time of 1 ms, resulting in an artificial decay of  $G_{GG}/G_{GR}$  for times larger than the bin time.

Therefore, we analyzed the measured  $G_{GG}/G_{GR}$  by comparison with simulated single-photon data. For the simulation, we used a simple model of freely

diffusing molecules possessing FRET with two energy transfer efficiencies ( $\langle E_{t,1} \rangle$  and  $\langle E_{t,2} \rangle$ ), with the simplification of equal interconversion rates ( $k_{12}=k_{21}$ ). This simplification is justified by the roughly equal area of the Gaussian peaks fitted to the  $E_{app}$  histogram (Fig. 1b).  $E_{t,1}$  and  $E_{t,2}$  have been chosen, referring to the peak positions of the two-Gaussian fit model of the experimental data ( $\langle E_{app,1} \rangle = 0.56$ ;  $\langle E_{app,2} \rangle = 0.88$ ; see Fig. 1b), but with a slight shift ( $\langle E_{t,1} \rangle = 0.50$ ;  $\langle E_{t,2} \rangle = 0.93$ ), which yields better matching of the amplitude of  $G_{GG}/G_{GR}$  between simulated and experimental data. Diffusion coefficient and further parameters (e.g., focus size) of the simulation have been adjusted to fit best to the experiment. The simulated data for different rates  $k_{12}=k_{21}$  were analyzed with the same procedure as was used for the experimental data.

The results of  $G_{GG}/G_{GR}$  are shown in Fig. 2a for *TtSlyD* and in conjunction with the simulated data. Additionally, the same analysis was applied to a control measurement of polyproline (Pro)<sub>20</sub> with identical dyes, comparable diffusion time of  $\tau_D = (185 \pm 5)$   $\mu$ s and with negligible intramolecular dynamics above the nanosecond timescale due to its stiff character.<sup>28,29</sup> The length of the polyproline ruler was 20 monomers, approximately matching the transfer efficiency obtained for *SlyD*.

For *TtSlyD*, there is a clear decay in  $G_{GG}/G_{GR}$  in the time range between 0.1 ms and 1 ms. To assure that the decay for *TtSlyD* is not an artifact due to diffusion effects that happen on a similar timescale [ $\tau_D = (180 \pm 5)$   $\mu$ s], we repeated the experiment with *TtSlyD* with an enlarged focus (by underfilling the microscope objective<sup>30</sup>), resulting in a twofold increased diffusion time [ $\tau_D = (\tau_D = 350 \pm 5)$   $\mu$ s]. For both focus sizes, the  $G_{GG}/G_{GR}$  curves coincide over the whole timescale up to the binning time of 1 ms.

In contrast to *TtSlyD*, the control does not show a pronounced decay, corroborating our conclusion that the measured  $G_{GG}/G_{GR}$  decay of *TtSlyD* is caused by internal dynamics. The measured decay of  $G_{GG}/G_{GR}$  for *TtSlyD* is best reproduced by the simulated data with interconversion rates between 50 Hz and 200 Hz. More accurate figures cannot be given due to the uncertainty of experimental values. However, we can suggest that there is intrinsic dynamics of *TtSlyD* on a timescale in the range of 100 Hz.

The question remains whether this dynamics can account for the observed broadening of the  $E_{app}$  histogram (Fig. 2b). Comparing the  $E_t$  histograms from the simulated data with the experimental  $E_{app}$  histogram clearly shows that, in the range of interconversion rates, which yield dynamics results matching those in the experiment, the simple two-state model is not sufficient to explain the broad distribution of energy transfer rates, even though increasing interconversion rates lead to merging

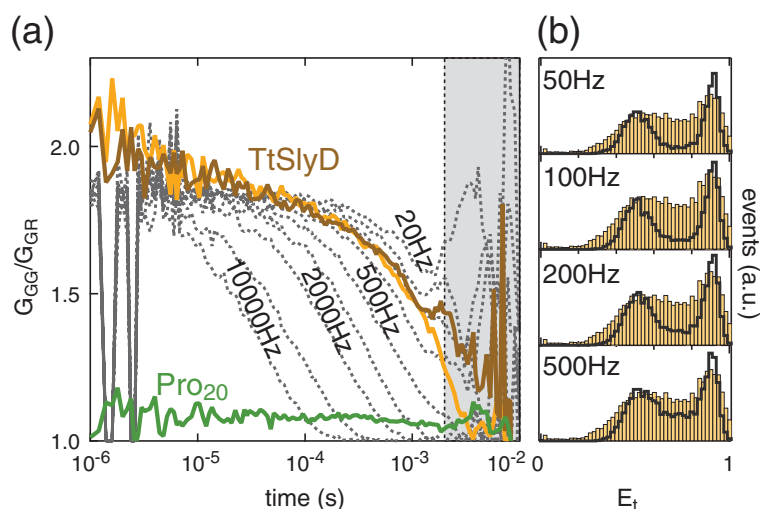


**Fig. 2.** Correlation and burst analysis of protein dynamics in comparison to simulated data. (a) The ratio  $G_{GG}/G_{GR}$  of burst-selected autocorrelation of the donor signal ( $G_{GG}$ ) and cross-correlation of the donor and acceptor signals ( $G_{GR}$ ) for *TtSlyD* in a diffraction-limited focus (brown line), in an enlarged focus (yellow line) and for the reference (Pro)<sub>20</sub> in trifluoroethanol (green line) during donor excitation (488 nm, 40  $\mu$ W). The focus is enlarged by underfilling the objective, resulting in twofold increased diffusion time of  $\tau_D = (350 \pm 5)$   $\mu$ s compared to  $\tau_D = (180 \pm 5)$   $\mu$ s in the small focus. The bursts are selected by a sum threshold of 40 cts/ms for

the total intensity during donor excitation and an additional threshold of 10 cts/ms for the acceptor intensity after direct excitation (635 nm, 10 MHz, 15  $\mu$ W). The same analysis was applied to simulated data of free diffusing molecules with  $\langle E_{t,1} \rangle = 0.50$  and  $\langle E_{t,1} \rangle = 0.88$  and equal interconversion rates on different timescales of 10 kHz to 20 Hz (broken lines). (b) Respective  $E_t$  histograms of the selected burst events of the simulated data with dynamics between 50 Hz and 500 Hz (black lines). For comparison, in every panel, the  $E_{app}$  histogram for the experimental data of *TtSlyD* in the diffraction-limited focus is shown (yellow bars).

peaks in the  $E_t$  histogram.<sup>26,31</sup> The FRET histogram can only be interpreted, assuming additional conformational plasticity superimposed to the two main conformational states.

### Conformational heterogeneity and dynamics upon ligand binding

To test whether ligand binding affects the revealed conformational heterogeneity, we performed experiments with *TtSlyD* in the presence of different protein substrates and inhibitors. The immunosuppressive agents FK506 and rapamycin act as inhibitors of the PPIase activity of FKBP.<sup>5,17,32</sup> With NMR titration experiments, it has been shown that these inhibitors of *TtSlyD* are interacting predominantly with amino acids in the active site of the FKBP domain of *TtSlyD* (M.K. and J.B., to be published elsewhere). As a substrate to monitor the PPIase activity, we used the reduced and carboxymethylated form of the S54G/P55N variant of ribonuclease T1 (RCM-T1).<sup>19,33</sup> Its refolding under high-salt conditions (2 M NaCl) is limited by the *cis*-to-*trans* isomerization reaction of Pro39,<sup>34</sup> which is catalyzed by the FKBP domain of *TtSlyD*.<sup>19</sup> Interestingly, Löw *et al.* also found that the  $k_{cat}/K_m$  value in the catalysis of RCM-T1 refolding by *TtSlyD* is increased by a factor of 100 as compared to a variant of *TtSlyD*, which lacks the IF domain.<sup>19</sup> That emphasizes the role of the IF domain. The experiments here were carried out under low-salt conditions (100 mM NaCl). Consequently, RCM-T1 remains permanently unfolded. However, we ex-

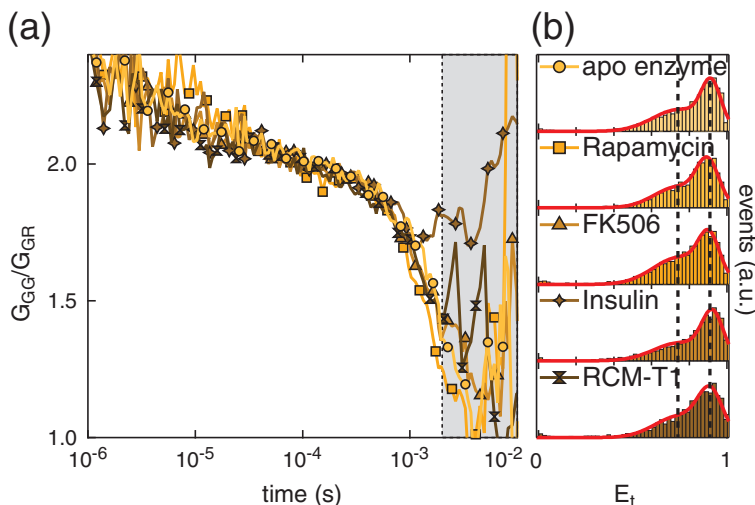
pect transient *cis*-*trans* isomerization reactions catalyzed by *TtSlyD*. For truncated SlyD\* of *E. coli* (which closely resembles *TtSlyD*<sup>19</sup>), Weininger *et al.* have shown that RCM-T1, as example for a permanently unfolded protein chain, binds to more than one binding site of SlyD\* with residues harboring both the IF domain and the FKBP domain.<sup>18</sup>

The standard method to measure the chaperone activity of the IF domain is an insulin aggregation assay.<sup>35,36</sup> We used insulin as ligand for the unspecific binding at the IF domain<sup>18,19</sup> with and without (data not shown) the reducing agent DTT.

For all experiments, the ligands were added in a concentration well above the dissociation constant  $K_d$ . Buffer and further experimental conditions were kept unchanged. Surprisingly, the  $E_{app}$  histograms do not significantly change (Fig. 3b). The shape remains broad, with indication of at least two subpopulations.

Only subtle changes in the relative contributions of the peaks representing the “closed” conformation (close to  $E_{app} = 1$ ) and the “open” conformation are observable. On the one hand, the closed conformation is enhanced after addition of insulin, whereas the closed conformation is reduced in the case of inhibitor binding of FK506.

Strikingly, also dynamics seems to be mostly unaffected by binding of the substrates or inhibitors. The  $G_{GG}/G_{GR}$  curves for all ligand experiments in Fig. 3a coincide. Independent of the presence of a binding partner, the characteristic decay between 0.1 ms and 1 ms is reproduced.



$E_{app}$  histograms are fitted with a two-Gaussian model (red line). The center positions of the two single components determined for the apoenzyme are indicated as black dotted lines.

## Discussion and Conclusion

Since the pioneering publication by Frauenfelder *et al.*,<sup>37</sup> the role of conformational dynamics for enzyme catalysis recently has been evidenced by numerous experiments. This development has been sparked by NMR investigations<sup>38–40</sup> and also by the advances in single-molecule methods, both from force detection via atomic force microscopy<sup>41</sup> or optical tweezers<sup>42,43</sup> and from single-molecule fluorescence methods.<sup>44</sup> smFRET has been proven particularly useful for the study of conformational heterogeneity and dynamics.<sup>24,26,27,45–51</sup>

In the present work, we aimed to elucidate the role of conformational flexibility and dynamics for the catalytic activity of a two-domain protein belonging to the family of FKBP PPIases. smFRET data clearly indicated that *TtSlyD* does not adopt a single, unique conformation. This finding is in accordance with recent results by NMR spectroscopy, where a defined relative orientation of the FKBP and IF domains toward each other could not be determined.<sup>18,20</sup> Further indication for flexibility between the two domains results from crystallographic studies, where the relative orientation of the two domains obtained from three different crystal structures varies significantly.<sup>19</sup> All of these studies, however, do not allow assessment of the energy landscape of the hinge motion. The shape of the transfer efficiency distribution, which in turn is representing a distance distribution, allows us to draw the conclusion that at least two main minima in this energy landscape must exist, which we call the open (for low FRET efficiency) and closed (for high FRET efficiency) states of the enzyme in analogy to other enzymes such as adenylate kinase.<sup>24</sup> Several

control experiments exclude significant contributions from the photophysics and local effects of the two dyes to the apparent  $E_{app}$  distribution. Therefore, we can attribute this observation to an intrinsic property of *TtSlyD*, which is conformational heterogeneity. The shape of the  $E_{app}$  histogram is indicative for the existence of additional conformational states beside the open and closed forms with local minima on the energy landscape. In view of the results from crystallography and NMR hydrogen/deuterium exchange, which is sensitive to local stability, this is not unexpected as, in particular, the IF domain seems to be very flexible or, in other terms, locally more disordered compared to the FKBP domain.<sup>19</sup> This observation was confirmed by NMR relaxation data for *E. coli* SlyD\*<sup>18,52</sup> and *TtSlyD*.<sup>52</sup> Although it is not advisable to extract absolute distances from the measured transfer efficiencies, a rough estimate gives 50 Å in the “open” state and 37 Å in the “closed” state. The distance in the open state is slightly larger than the distance of the C $^{\alpha}$  atoms in Fig. 1a, which can be attributed to the additional distance from the linker length.

One limitation of the structural investigations in the crystal is the lack of dynamics information, that is, on which timescale the relative global motion of the two domains occurs. Dynamic NMR analyses are limited on a timescale of 50 ns to 1 ms and if relative domain motions do not cause local chemical shift changes. Already from the FRET efficiency histograms it can be deduced that the transfer efficiency and thus the distance cannot exchange much faster than the dwell time of the molecule in the detection region of about 100  $\mu$ s. The efficiency histogram is compatible even with static conformational heterogeneity, that is, different but non-converting

**Fig. 3.** Analysis of interactions with protein substrates and inhibitors. (a) Normalized  $G_{GG}/G_{GR}$  quotient for *TtSlyD* in native buffer without any ligand (circles), with 70  $\mu$ M rapamycin (squares), with 100  $\mu$ M FK506 (triangles), with 200  $\mu$ M insulin (stars) and with 14  $\mu$ M RCM-T1 (double triangles). The bursts are selected by a sum threshold of 40 cts/ms for the total intensity during donor excitation and an additional threshold of 10 cts/ms for the acceptor intensity after direct excitation (635 nm, 10 MHz, 15  $\mu$ W). (b) Respective  $E_{app}$  histograms of the selected burst events under different ligand conditions. The

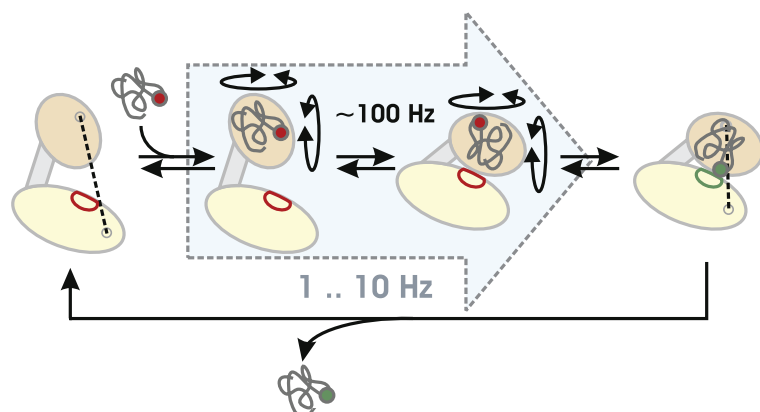


**Fig. 4.** Cartoon of the proposed mechanism involving conformational dynamics in the search for the chemical step, which is a *cis trans* isomerization of a prolyl-peptidyl bond (red/green dot) in the substrate (coiled chain). The substrate bound to the IF domain (light red) is exposed several times to the active site (red circle) in the FKBP domain (yellow) with some additional flexibility, enhancing the chance for favorable alignment. Eventually, the substrate is released from the IF domain.

conformations. Correlation analysis has been proven useful for the study of microsecond conformational dynamics.<sup>53–55</sup> Here, we used a method introduced by Torres and Levitus, which allows us to assess conformational dynamics on much longer timescales.<sup>23</sup> With this method, Santoso *et al.* determined the rate of conformational exchange of DNA polymerase I in polyacrylamide gels.<sup>26</sup> Our approach is slightly different because we apply the correlation analysis only to bursts in order to be able, first, to select correctly labeled proteins only and, second, to reduce background contributions. Furthermore, we compared simulated and experimental data instead of fitting to a stretched exponential for the estimation of the rate of conformational dynamics. This shows that even assuming a single rate of conversion between the conformationally distinct states, simulated data reproduce the experimental observations quite well. The best agreement is achieved for a rate of about 200 Hz. While the correlation function is well reproduced by a simulation with just two conformational states, the transfer efficiency histogram is not, leading us to the conclusion that the events between the main peaks in the transfer efficiency distribution are not due to averaging of transitions.<sup>26</sup>

In order to elucidate the role of conformational dynamics to catalysis, we performed smFRET experiments also in the presence of different binding partners of *TtSlyD*. FK506 and rapamycin are inhibitors of the PPIase activity and bind to the FKBP domain, whereas RCM-T1 is a substrate for the PPIase activity. Insulin, on the other hand, is used in an assay for testing the chaperone activity. The finding that neither of the binding partners (inhibitors of the FKBP domain and substrates binding to both the chaperone and the FKBP domain) seems to significantly change the conformational equilibrium first comes as a surprise because such a change was clearly evident in the case of AdK<sup>24</sup> and DNA polymerase I.<sup>26</sup> These two enzymes, however, are highly specific, and the substrates are small molecules, in contrast to *SlyD*,

which binds large substrates with low specificity. *SlyD* from different organisms have also all in common that the substrate and inhibitor affinities are moderate in the low micromolar range (e.g., for *EcSlyD*, the  $K_m$  constant for RCM-T1 is 1.7  $\mu\text{M}$ , and the  $K_i$  for unfolded protein substrates is 0.2–2.3  $\mu\text{M}$  and for FK506 is 4.6  $\mu\text{M}$ ).<sup>17</sup> These low affinities are in line with our observation of negligible influence of substrate or inhibitor binding onto the conformational equilibrium and dynamics. Careful binding studies on *EcSlyD* recently also showed that binding of unfolded proteins to the IF domain does not strongly interfere with binding at the prolyl isomerase site.<sup>56</sup> Note, that inhibitors of *TtSlyD* and substrate binding were analyzed in the present study under equilibrium conditions, where RCM-T1 does not fold. Under net turnover conditions, changes in the conformational equilibrium might occur.

Based on our findings, we propose an extended mechanistic model for the catalysis by *SlyD* as compared to the model established by Jakob *et al.*, which is shown as a cartoon in Fig. 4.<sup>16</sup> Unfolded or partially unfolded polypeptide chains first bind to the IF chaperone domain, which has been confirmed by, for example, NMR titration.<sup>19</sup> The repetitive motion toward the FKBP domain increases the local concentration and thereby increases the chance that the peptidyl-prolyl bond is close to the active site of the FKBP domain. The earlier proposed model by Jakob *et al.* assumes that  $k_{\text{cat}}$  is limited by the dissociation from the IF domain and transfer to the FKBP domain, before the actual isomerization at the FKBP occurs, which is a much faster process.<sup>16</sup> Our findings suggest that it is more likely that the substrate remains bound to the IF domain during catalysis. The structural flexibility allows the enzyme to sample different orientations of the substrate relative to the FKBP domain with a rate of about 200 Hz. Such a mechanism also enables a variety of substrates to be catalyzed rather unspecifically and without a high affinity for the active site of the PPIase, which are both properties of *SlyD*.

Consequently, release from the IF domain and subsequent binding to the FKBP domain are not necessary to achieve catalysis. This extension of the enzyme mechanism is based on the here presented experimental observation that the presence of substrates of SlyD and inhibitors of the FKBP domain does not significantly change the conformational partitioning into an open and closed states and their rate of interconversion. The exchange of substrates probably occurs in the open conformation, that is, when the distance between the IF and FKBP domains is large. Still, the rate-limiting step in catalysis is the release of the substrate from the IF domain, resulting in a  $k_{\text{cat}}$  of about 1 Hz generally found for protein substrates of SlyD from different species.<sup>16,17</sup> The functionally, and from the domain structure, related trigger factor shows a rate constant of about 8 Hz for the same release.<sup>57</sup> Note, that this release in our proposed model is not used for the transfer of the substrate to the PPIase active site but is used for the release of the substrate after successful isomerization. As mentioned, the isomerization itself is rather fast, as a  $k_{\text{cat}}$  value of 600 Hz was found for Leu-Pro isomerization in a tetrapeptide.<sup>16</sup> The mechanism proposed here is potentially general because it is similar to a mechanism also proposed, entirely based on NMR experiments,<sup>13</sup> for sFkpA, a related protein with a PPIase and a chaperone domain. One can speculate that this mechanism is involved in catalysis by many other enzymes exhibiting high substrate promiscuity.

## Materials and Methods

Expression, purification and labeling were performed according to standard protocols.<sup>19,24</sup> Single-molecule experiments were conducted on a home-built confocal optical microscope<sup>24</sup> equipped with a continuous-wave solid-state laser operating at 488 nm (Spectra Physics Cyan; Newport Corporation, Irvine, CA, USA) and a pulsed diode operating at 470 nm, respectively, to excite the donor and a pulsed diode laser operating at 635 nm to excite the acceptor laser (LDH-P-C-470 and LDH-P-C-635; PicoQuant GmbH, Berlin, Germany). Excitation and fluorescence collection were achieved by a N.A.=1.2 water immersion microscope objective (CFI Plan Apochromat 60× WI; Nikon, Japan), and fluorescence was detected by avalanche photo diodes (SPCM-AQ 14; PerkinElmer, Waltham, MA, USA). Dedicated counting electronics (TimeHarp 200; PicoQuant GmbH) recorded the photon arrival times, and data were analyzed with home-written procedures in Igor Pro (WaveMetrics, Portland, OR, USA). For smFRET experiments, the samples were diluted in sample buffer [50 mM sodium phosphate (pH 7.5) and 100 mM sodium chloride] to a concentration of about 100 pM. Additionally, all samples contained 0.001% (w/v) Tween 20 (Carl Roth GmbH, Karlsruhe, Germany) to prevent surface adhesion of the protein. Additionally, the cover slides were passivated with a spin-coated layer of poly(methyl methacrylate) (Goodfellow

GmbH, Bad Nauheim, Germany). More details are presented in Supporting Material.

---



---

## Acknowledgement

We thank U. Weininger for many helpful discussions. This research was supported by grants from the Volkswagen foundation (AZ I/83 019) and the Deutsche Forschungsgemeinschaft (SFB 610 and GRK 1026).

## References

- Eaton, W. A., Munoz, V., Hagen, S. J., Jas, G. S., Lapidus, L. J., Henry, E. R. & Hofrichter, J. (2000). Fast kinetics and mechanisms in protein folding. *Annu. Rev. Biophys. Biomol. Struct.* **29**, 327–359.
- Dobson, C. M. (2003). Protein folding and misfolding. *Nature*, **426**, 884–890.
- Schmid, F. X., Mayr, L. M., Mücke, M. & Schönbrunner, E. R. (1993). Prolyl isomerases: role in protein folding. *Adv. Protein Chem.* **44**, 25–66.
- Fischer, G. (1994). Peptidyl-prolyl *cis/trans* isomerases and their effectors. *Angew. Chem., Int. Ed. Engl.* **33**, 1415–1436.
- Göthel, S. F. & Marahiel, M. A. (1999). Peptidyl-prolyl *cis/trans* isomerases, a superfamily of ubiquitous folding catalysts. *Cell. Mol. Life Sci.* **55**, 423–436.
- Walter, S. & Buchner, J. (2002). Molecular chaperones – cellular machines for protein folding. *Angew. Chem., Int. Ed. Engl.* **41**, 1098–1113.
- Harrison, R. K. & Stein, R. L. (1990). Substrate specificities of the peptidyl prolyl *cis/trans* isomerase activities of cyclophilin and FK-506 binding protein: evidence for the existence of a family of distinct enzymes. *Biochemistry*, **29**, 3813–3816.
- Hesterkamp, T. & Bukau, B. (1996). The *Escherichia coli* trigger factor. *FEBS Lett.* **389**, 32–34.
- Scholz, C., Stoller, G., Zarnit, T., Fischer, G. & Schmid, F. X. (1997). Cooperation of enzymatic and chaperone functions of trigger factor in the catalysis of protein folding. *EMBO J.* **16**, 54–58.
- Ludlam, A. V., Moore, B. A. & Xu, Z. (2004). The crystal structure of ribosomal chaperone trigger factor from *Vibrio cholerae*. *Proc. Natl. Acad. Sci. USA*, **101**, 13436–13441.
- Webb, H. M., Ruddock, L. W., Marchant, R. J., Jonas, K. & Klappa, P. (2001). Interaction of the periplasmic peptidylprolyl *cis/trans* isomerase SurA with model peptides. The N-terminal region of SurA is essential and sufficient for peptide binding. *J. Biol. Chem.* **276**, 45622–45627.



12. Xu, X., Wang, S., Hu, Y. X. & McKay, D. B. (2007). The periplasmic bacterial molecular chaperone SurA adapts its structure to bind peptides in different conformations to assert a sequence preference for aromatic residues. *J. Mol. Biol.* **373**, 367–381.
13. Hu, K., Galius, V. & Pervushin, K. (2006). Structural plasticity of peptidyl prolyl isomerase sFkpA is a key to its chaperone function as revealed by solution NMR. *Biochemistry*, **45**, 11983–11991.
14. Suzuki, R., Nagata, K., Yumoto, F., Kawakami, M., Nemoto, N., Furutani, M. *et al.* (2003). Three-dimensional solution structure of an archaeal FKBP with a dual function of peptidyl prolyl *cis trans* isomerase and chaperone-like activities. *J. Mol. Biol.* **328**, 1149–1160.
15. Knappe, T. A., Eckert, B., Schaarschmidt, P., Scholz, C. & Schmid, F. X. (2007). Insertion of a chaperone domain converts FKBP12 into a powerful catalyst of protein folding. *J. Mol. Biol.* **368**, 1458–1468.
16. Jakob, R. P., Zoldak, G., Aumüller, T. & Schmid, F. X. (2009). Chaperone domains convert prolyl isomerases into generic catalysts of protein folding. *Proc. Natl. Acad. Sci. USA*, **106**, 20282–20287.
17. Scholz, C., Eckert, B., Hagn, F., Schaarschmidt, P., Balbach, J. & Schmid, F. X. (2006). SlyD proteins from different species exhibit high prolyl isomerase and chaperone activities. *Biochemistry*, **45**, 20–33.
18. Weininger, U., Haupt, C., Schweimer, K., Graubner, W., Kovermann, M., Brüser, T. *et al.* (2009). NMR solution structure of SlyD from *Escherichia coli*: spatial separation of prolyl isomerase and chaperone function. *J. Mol. Biol.* **387**, 295–305.
19. Löw, C., Neumann, P., Tidow, H., Weininger, U., Haupt, C., Friedrich-Epler, B. *et al.* (2010). Crystal structure determination and functional characterization of the metallochaperone SlyD from *Thermus thermophilus*. *J. Mol. Biol.* **398**, 375–390.
20. Martino, L., He, Y., Hands-Taylor, K. L., Valentine, E. R., Kelly, G., Giancola, C. & Conte, M. R. (2009). The interaction of the *Escherichia coli* protein SlyD with nickel ions illuminates the mechanism of regulation of its peptidyl-prolyl isomerase activity. *FEBS J.* **276**, 4529–4544.
21. Lakowicz, J. R. (2006). *Principles of Fluorescence Spectroscopy*, 3rd edit. Springer, New York, NY.
22. Förster, T. (1948). Zwischenmolekulare Energiewanderung und Fluoreszenz. *Ann. Phys.* **437**, 55–75.
23. Torres, T. & Levitus, M. (2007). Measuring conformational dynamics: a new FCS-FRET approach. *J. Phys. Chem. B*, **111**, 7392–7400.
24. Henzler-Wildman, K. A., Thai, V., Lei, M., Ott, M., Wolf-Watz, M., Fenn, T. *et al.* (2007). Intrinsic motions along an enzymatic reaction trajectory. *Nature*, **450**, 838–844.
25. Eggeling, C., Widengren, J., Brand, L., Schaffer, J., Felekyan, S. & Seidel, C. A. (2006). Analysis of photobleaching in single-molecule multicolor excitation and Förster resonance energy transfer measurements. *J. Phys. Chem. A*, **110**, 2979–2995.
26. Santoso, Y., Joyce, C. M., Potapova, O., Le Reste, L., Hohlbein, J., Torella, J. P. *et al.* (2010). Conformational transitions in DNA polymerase I revealed by single-molecule FRET. *Proc. Natl. Acad. Sci. USA*, **107**, 715–720.
27. Margittai, M., Widengren, J., Schweinberger, E., Schroder, G. F., Felekyan, S., Hausteiner, E. *et al.* (2003). Single-molecule fluorescence resonance energy transfer reveals a dynamic equilibrium between closed and open conformations of syntaxin 1. *Proc. Natl. Acad. Sci. USA*, **100**, 15516–15521.
28. Schuler, B., Lipman, E. A. & Eaton, W. A. (2002). Probing the free-energy surface for protein folding with single-molecule fluorescence spectroscopy. *Nature*, **419**, 743–747.
29. Nettels, D., Gopich, I. V., Hoffmann, A. & Schuler, B. (2007). Ultrafast dynamics of protein collapse from single-molecule photon statistics. *Proc. Natl. Acad. Sci. USA*, **104**, 2655–2660.
30. Enderlein, J., Gregor, I., Patra, D., Dertinger, T. & Kaupp, U. B. (2005). Performance of fluorescence correlation spectroscopy for measuring diffusion and concentration. *ChemPhysChem*, **6**, 2324–2336.
31. Gopich, I. V. & Szabo, A. (2007). Single-molecule FRET with diffusion and conformational dynamics. *J. Phys. Chem. B*, **111**, 12925–12932.
32. Kang, C. B., Hong, Y., Dhe-Paganon, S. & Yoon, H. S. (2008). FKBP family proteins: immunophilins with versatile biological functions. *NeuroSignals*, **16**, 318–325.
33. Mücke, M. & Schmid, F. X. (1994). Folding mechanism of ribonuclease T1 in the absence of the disulfide bonds. *Biochemistry*, **33**, 14608–14619.
34. Kiefhaber, T., Grunert, H. P., Hahn, U. & Schmid, F. X. (1990). Replacement of a *cis* proline simplifies the mechanism of ribonuclease T1 folding. *Biochemistry*, **29**, 6475–6480.
35. Scheibel, T., Weikl, T. & Buchner, J. (1998). Two chaperone sites in Hsp90 differing in substrate specificity and ATP dependence. *Proc. Natl. Acad. Sci. USA*, **95**, 1495–1499.
36. Haslbeck, M., Walke, S., Stromer, T., Ehrnsperger, M., White, H. E., Chen, S. *et al.* (1999). Hsp26: a temperature-regulated chaperone. *EMBO J.* **18**, 6744–6751.
37. Frauenfelder, H., Sligar, S. G. & Wolynes, P. G. (1991). The energy landscapes and motions of proteins. *Science*, **254**, 1598–1603.
38. Henzler-Wildman, K. & Kern, D. (2007). Dynamic personalities of proteins. *Nature*, **450**, 964–972.
39. Sugase, K., Dyson, H. J. & Wright, P. E. (2007). Mechanism of coupled folding and binding of an intrinsically disordered protein. *Nature*, **447**, 1021–1025.
40. Boehr, D. D., Dyson, H. J. & Wright, P. E. (2008). Conformational relaxation following hydride transfer plays a limiting role in dihydrofolate reductase catalysis. *Biochemistry*, **47**, 9227–9233.
41. Alegre-Cebollada, J., Perez-Jimenez, R., Kosuri, P. & Fernandez, J. M. (2010). Single-molecule force spectroscopy approach to enzyme catalysis. *J. Biol. Chem.* **285**, 18961–18966.
42. Abbondanzieri, E. A., Greenleaf, W. J., Shaevitz, J. W., Landick, R. & Block, S. M. (2005). Direct observation of base-pair stepping by RNA polymerase. *Nature*, **438**, 460–465.
43. Chemla, Y. R., Aathavan, K., Michaelis, J., Grimes, S., Jardine, P. J., Anderson, D. L. & Bustamante, C. (2005). Mechanism of force generation of a viral DNA packaging motor. *Cell*, **122**, 683–692.

44. Michalet, X., Weiss, S. & Jäger, M. (2006). Single-molecule fluorescence studies of protein folding and conformational dynamics. *Chem. Rev.* **106**, 1785–1813.
45. Rothwell, P. J., Berger, S., Kensch, O., Felekyan, S., Antonik, M., Wohrl, B. M. *et al.* (2003). Multiparameter single-molecule fluorescence spectroscopy reveals heterogeneity of HIV-1 reverse transcriptase: primer/template complexes. *Proc. Natl. Acad. Sci. USA*, **100**, 1655–1660.
46. Hanson, J. A., Duderstadt, K., Watkins, L. P., Bhattacharyya, S., Brokaw, J., Chu, J. W. & Yang, H. (2007). Illuminating the mechanistic roles of enzyme conformational dynamics. *Proc. Natl. Acad. Sci. USA*, **104**, 18055–18060.
47. Cornish, P. V., Ermolenko, D. N., Staple, D. W., Hoang, L., Hickerson, R. P., Noller, H. F. & Ha, T. (2009). Following movement of the L1 stalk between three functional states in single ribosomes. *Proc. Natl. Acad. Sci. USA*, **106**, 2571–2576.
48. Zhang, Z., Spiering, M. M., Trakselis, M. A., Ishmael, F. T., Xi, J., Benkovic, S. J. & Hammes, G. G. (2005). Assembly of the bacteriophage T4 primosome: single-molecule and ensemble studies. *Proc. Natl. Acad. Sci. USA*, **102**, 3254–3259.
49. Smiley, R. D., Collins, T. R., Hammes, G. G. & Hsieh, T. S. (2007). Single-molecule measurements of the opening and closing of the DNA gate by eukaryotic topoisomerase II. *Proc. Natl. Acad. Sci. USA*, **104**, 4840–4845.
50. Huang, F., Rajagopalan, S., Settanni, G., Marsh, R. J., Armoogum, D. A., Nicolaou, N. *et al.* (2009). Multiple conformations of full-length p53 detected with single-molecule fluorescence resonance energy transfer. *Proc. Natl. Acad. Sci. USA*, **106**, 20758–20763.
51. Ratzke, C., Mickler, M., Hellenkamp, B., Buchner, J. & Hugel, T. (2010). Dynamics of heat shock protein 90 C-terminal dimerization is an important part of its conformational cycle. *Proc. Natl. Acad. Sci. USA*, **107**, 16101–16106.
52. Kovermann, M., Zierold, R., Haupt, C., Löw, C. & Balbach, J. (2011). NMR relaxation unravels interdomain crosstalk of the two domain prolyl isomerase and chaperone SlyD. *Biochim. Biophys. Acta*, **1814**, 873–881.
53. Chattopadhyay, K., Elson, E. L. & Frieden, C. (2005). The kinetics of conformational fluctuations in an unfolded protein measured by fluorescence methods. *Proc. Natl. Acad. Sci. USA*, **102**, 2385–2389.
54. Neuweiler, H., Johnson, C. M. & Fersht, A. R. (2009). Direct observation of ultrafast folding and denatured state dynamics in single protein molecules. *Proc. Natl. Acad. Sci. USA*, **106**, 18569–18574.
55. Doose, S., Neuweiler, H., Barsch, H. & Sauer, M. (2007). Probing polyproline structure and dynamics by photoinduced electron transfer provides evidence for deviations from a regular polyproline type II helix. *Proc. Natl. Acad. Sci. USA*, **104**, 17400–17405.
56. Zoldák, G. & Schmid, F. X. (2011). Cooperation of the prolyl isomerase and chaperone activities of the protein folding catalyst SlyD. *J. Mol. Biol.* **406**, 176–194.
57. Maier, R., Scholz, C. & Schmid, F. X. (2001). Dynamic association of trigger factor with protein substrates. *J. Mol. Biol.* **314**, 1181–1190.